

Low Complexity Detect and Avoid for Autonomous Agents in Cluttered Environments

Mosab Diab
Delft University of Technology (TUD)
Faculty of EEMCS, Mekelweg 4
2628 CD Delft, The Netherlands

Mostafa Mohammadkarimi
Delft University of Technology (TUD)
Faculty of EEMCS, Mekelweg 4
2628 CD Delft, The Netherlands

Raj Thilak Rajan
Delft University of Technology (TUD)
Faculty of EEMCS, Mekelweg 4
2628 CD Delft, The Netherlands

Abstract—In this paper, we propose a fast and low complexity detect and avoid (DAA) algorithm for unknown cluttered environments. Examples of such scenarios include but are not limited to various terrestrial missions e.g., search and rescue missions in jungles, and in space-exploration e.g., navigation of rovers on the Moon. The proposed method is based on the concept of artificial potential fields (APF) in which the target is attractive while the obstacles are repulsive to the mobile agent. To the original APF algorithm (by Khatib), we propose two major updates which significantly improve the performance of DAA using APF. First, we propose to improve an existing classical method that replaces the gradient descent optimization of the potential field cost function on a continuous domain with a combinatorial optimization on a set of predefined points (called bacteria points) around the agent’s current location. Our proposition includes an adaptive hyperparameter that changes the value of the potential function associated to each bacteria point based on the current environmental measurements. Our proposed solution improves the navigation performance in terms of convergence to the target at the expense of minimal increase in computational complexity. Second, we propose an improved potential field cost function of the bacteria points by introducing a new branching cost function which further improves the navigation performance. The algorithms were tested on a set of Monte Carlo simulation trials where the environment changes for each trial. Our simulation results show 25% lower navigation time and around 200% higher success rate compared to the conventional potential field method.

TABLE OF CONTENTS

1. INTRODUCTION.....	1
2. SYSTEM MODEL.....	2
3. ARTIFICIAL POTENTIAL FIELDS (APF)	2
4. IMPROVED BACTERIA APF (IBAPF) ALGORITHMS	4
5. SIMULATIONS	5
6. SUMMARY	7
REFERENCES	7

1. INTRODUCTION

According to the Food and Agriculture Organization (FAO), jungles and forests cover about 4.06 billion hectares which is about 31% of the global land area of Earth [1]. These areas generate around 86 million jobs, and the lives of many people depend on that [1]. While agricultural robots have hundreds of applications around the world in recent years, the

applications of robots in forests and jungles have been limited to overhead surveillance and mapping. The reason for this disparity can be attributed to the fact that forest environments are generally more complex than agricultural environments. The highly unstructured and steep slope terrains in addition to the variations in temperature and humidity make it difficult to develop robust robotic systems. There is also no communication infrastructure in remote forests, and communication links are obstructed by the dense vegetation which adds to the challenge. Forest robots need special hardware and locomotion systems to operate in these environments where there is no protection against storms [2].

Forests are just one example of an unknown cluttered environment that a robot needs an intelligent navigation system; another example is subaquatic environments. The National Oceanic and Atmospheric Administration (NOAA) estimates that about 95% of the world’s oceans and 99% of the ocean floor are yet needed to be explored [3]. The dense vegetation that lies underneath the surface of the ocean such as coral reefs and seaweed as well as the dwelling creatures add to the challenges of exploration. Autonomous agents are essential to underwater exploration and collection of samples due to their ability to survive longer than human agents on short missions.

Robot applications in jungles and forests include but are not limited to: monitoring and surveillance for environmental preservation and security, forest planting and harvesting, and wildfire firefighting. The applications of underwater robots span a wide range from monitoring marine life to removal of underwater sea mines.

Autonomous agents such as drones and rovers are the future of delivery systems, search and rescue missions, and surveillance systems. The navigation systems for drones in unknown and cluttered environments like jungles, oceans, and sea floors are in their early development stages and still don’t have the sufficient performance levels to be deployed into the field. Specifically, low complexity detect and avoid (DAA) algorithms are needed to be developed for autonomous agents.

In this paper we propose a DAA algorithm optimized for cluttered environments that outperforms existing low complexity DAA algorithms in terms of convergence and time it takes to navigate. We first start by analyzing the existing DAA methods and deciding which one is the most suitable for use in cluttered environments. We then define our system model and describe the artificial potential field (APF) method. After that, the DAA system developed for cluttered environments is described along with the contributions we made. We then

discuss the local minima trap which is the biggest drawback of APF methods. We conclude the paper with the simulation setup and results.

Related Research

The working principle of existing collision avoidance systems can be explained by either reactive control or deliberative planning. Reactive control is when the agent gathers information using on-board sensors and reacts based on the gathered data. Reactive control allows for rapid response but can lead to a corner case in the path and might get the agent stuck so it may need another technique combined with it in order to avoid that. Deliberative planning on the other hand is when there is an environmental map that is constantly updated by the agent. Then, the optimal collision free navigation path is calculated. The latter method needs an accurate map of the environment and that is computationally extensive specially for a dynamic environment. A hybrid approach between the two is considered more suitable for dynamic environments [4].

Existing collision avoidance methods can be divided into four groups:

1. Geometric Methods
2. Force-Field Methods
3. Optimisation-Based Methods
4. Sense-and-Avoid Methods

Comparison Between Methods—Multiple parameters can be used for performance comparison of DAA methods. In this section, we will review some of these methods and try to indicate the discrepancy.

The real time performance of the sense and avoid and geometric methods is better than the force-field and optimisation methods [4, p. 11]. Sense and avoid does not increase computational complexity if a change happens in the environment such as an obstacle moving [5]. Geometric methods are also computationally light but are highly dependent on the algorithm implementation in terms of computation time [6]. Optimisation methods are of medium complexity while the force-field methods are considered low-complex in implementation [4, p. 11]. The velocity constraint is a metric that takes the velocity of the obstacles in consideration. Sense and avoid and geometric approaches are capable to handle this constraint well [7],[8]. However, force-field and optimisation methods are better for predefined planning which does not take changing dynamics into consideration [4, p. 11]. The third metric is static and dynamic environment suitability. For dynamic environments, sense and avoid is the easiest and lightest due to the local computations being performed on board the agent through the changes observed by the sensory system on the agent itself [9]. Geometric methods give an acceptable performance but less optimal than sense and avoid [10]. Force-field methods do not perform well in narrow passages and can lead to a local minima trap in dynamic environments [11]. Optimisation methods are more suitable for static environments as they require pre-planning and have to optimise the whole route again in case a change is detected [4, pp. 11-12].

When it comes to deadlock, the geometrical and optimisation methods don't have this issue due to the fact that they are designed for known structured environments. Force-field methods can get stuck in a local minima. Sense and avoid methods can reach a deadlock and require another methodology for handling this issue as it can't be solved locally [4, p. 12].

When it comes to swarm compatibility all the approaches can be applied to a swarm of agents but might need an additional algorithm for handling communication between the agents. When it comes to dimensionality, all the mentioned methods need some minor modifications when it comes to scaling the algorithms developed for 2D to handle 3D environments. However, there is current research on the feasibility of force-field methods for 3D dynamic environments [4],[12]. For pre-mission path planning, sense and avoid and force field methods do not require that because the plan is made when the obstacle is detected in-flight. Optimisation and geometric methods on the other hand, require path planning beforehand as the obstacle locations need to be known to the UAV before encountering the obstacles.

The takeaway point here is that for unknown cluttered environments, the force-field method is the best one to use. The reason for that is that the geometric and optimisation methods are designed for known structured environments and do not perform well in unknown cluttered environments while the sense and avoid methods do not take multiple obstacles into account which is necessary for cluttered environments.

2. SYSTEM MODEL

We consider an agent with a known position $\mathbf{r} = [x, y]^T$ which aims to navigate through a set of N cluttered static obstacles in a $2D^2$ environment to a target of a known location $\mathbf{r}_t = [x_t, y_t]^T$. The agent uses dead reckoning technique to obtain its location during navigation [13]. It is assumed that the number and location of the obstacles are unknown to the agent. The location of the obstacles are considered to be a random vector uniformly distributed in a rectangular environment with length L_x and L_y . The agent starts the navigation from a known location $\mathbf{r}_s = [x_s, y_s]^T$ and it is equipped with an ultrasonic sensor that measures the distance to the obstacles. The distance to obstacles is achieved by measuring round trip time of arrival (TOA) of the ultrasonic signal.

The detection range of the agent's sensor is denoted by ρ_{rn} . The agent can detect only the obstacles within its detection range in each navigation step. Thus, the number of detected obstacles varies during navigation. The navigation is composed of a measurement step followed by path planning, where it is finding a geometrical path from the current location of the agent to its next location while avoiding obstacles in the environment.

3. ARTIFICIAL POTENTIAL FIELDS (APF)

In this section, we briefly overview APF methods that are promising for DAA in unknown cluttered environments. In general, the APF methods works on the basis that a target is attractive while an obstacle is repulsive. The agent is to be attracted by the goal point and hence moves towards it while changing direction whenever an obstacle is encountered. An example for this is a mobile electrical charge moving in a field of static similar charges while being attracted by a static opposite charge. The advantage of this method is that it takes into account the effect of multiple obstacles at once which makes it perfect for cluttered environments which are the scope of this research.

²Extension to 3D case is straightforward.

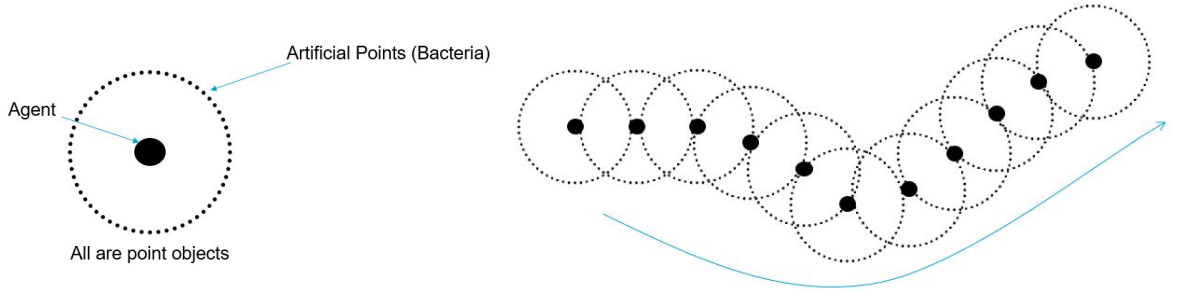


Figure 1: Agent and bacteria points around it (left) Agent movement by selecting different bacteria points (right).

Classical APF (CAPF) Algorithm

The original APF method proposed in 1985 [14] uses geometric calculations at each iteration to determine the direction and speed the agent should move on in order to avoid the obstacles and reach the target safely. It was originally proposed for robotic arm manipulators but has been extended to mobile agents afterwards [15].

The CAPF method was originally designed for structured environments. It can still work in cluttered environments but is far from optimal and often gets stuck in local minimas and collide with obstacles. Hence, the need arises for a new method that is dedicated for cluttered environments and that is the purpose of this paper.

Classical Bacteria APF (BAPF) Algorithm

The principle idea of the classical BAPF method for autonomous navigation is illustrated in Figure 1 and is adopted from [16]. As seen, it is based on the idea of having a point agent surrounded by a circle of possible position points called bacteria points. There are potential functions that are calculated for those points based on the distance from the target and from the detected obstacles. Based on those potential functions a certain bacteria point is selected to be the next position of the agent, and the agent moves to it. This process is repeated during navigation [16]. This method shall overcome the limitations that the CAPF method faces when it comes to unknown cluttered environments [15].

In the classical BAPF algorithm, the potential function from the target located at $\mathbf{r}_t = [x_t, y_t]^T$ to the agent located at $\mathbf{r} = [x, y]^T$ is given by

$$J_t(\mathbf{r}) \triangleq -\alpha_t \exp(-\mu_t \rho_t(\mathbf{r})), \quad (1)$$

where $\rho_t(\mathbf{r}) \triangleq \|\mathbf{r} - \mathbf{r}_t\|_2^2$ is the square distance between the agent and target, and α_t and μ_t are constant parameters empirically determined based on the size of the environment and the initial distance between the agent and the target.

Similarly, the repulsive potential function from the n th detected obstacle located at $\mathbf{r}_{\text{obst}}^n = [x_{\text{obst}}^n, y_{\text{obst}}^n]^T$ to the agent located at $\mathbf{r} = [x, y]^T$ is defined as

$$J_{\text{obst}}^n(\mathbf{r}) \triangleq \alpha_o \exp(-\mu_o \rho_{\text{obst}}^n(\mathbf{r})) \quad (2)$$

where $\rho_{\text{obst}}^n(\mathbf{r}) \triangleq \|\mathbf{r} - \mathbf{r}_{\text{obst}}^n\|_2^2$ is the square distance between the agent and the n th obstacle, and α_o and μ_o are constant parameters determined through experimentation based on the estimated density of obstacles in the navigation region.

Let N_d denote the total number of detected obstacles by the agent at the location of $\mathbf{r} = [x, y]^T$. The total repulsive potential function from the N_d detected obstacles at the location of the agent $\mathbf{r} = [x, y]^T$ is given by

$$J_{\text{obst}}(\mathbf{r}) = \sum_{n=1}^{N_d} J_{\text{obst}}^n(\mathbf{r}), \quad (3)$$

where $J_{\text{obst}}^n(\mathbf{r})$ is given in (2). By using (1) and (3), the total potential function at the agent's location $\mathbf{r} = [x, y]^T$ can be written as

$$J_a(\mathbf{r}) = J_t(\mathbf{r}) + J_{\text{obst}}(\mathbf{r}). \quad (4)$$

Let N_b and $\mathbf{r}_{b,k} = [x_{b,k}, y_{b,k}]^T$, $k = 1, 2, \dots, N_b$, denote the total number of bacteria points and the location of the k th bacteria point around $\mathbf{r} = [x, y]^T$ respectively. The total potential function at the location of the k th bacteria point around $\mathbf{r} = [x, y]^T$ is expressed as

$$J_k(\mathbf{r}_{b,k}) = J_t(\mathbf{r}_{b,k}) + J_{\text{obst}}(\mathbf{r}_{b,k}). \quad (5)$$

The criteria for the movement of the agent located at $\mathbf{r} = [x, y]^T$ to the k th bacteria point at $\mathbf{r}_{b,k} = [x_{b,k}, y_{b,k}]^T$ is given by

$$J_k(\mathbf{r}_{b,k}) - J_a(\mathbf{r}) < 0, \quad (6)$$

which means that the k th bacteria point is at a lower total potential towards the target than the agent. Recall from (1) and (2) that the target potential is negative while the repulsive potential from the obstacles is positive.

Figure 2 illustrates the block diagram of the classical BAPF algorithm. As seen, a linear search algorithm on the bacteria points is performed to select the best bacteria point to move to. The block diagram of the search algorithm is shown in Figure 3. As seen, the search starts with testing the bacteria point closest to the target. If that point meets the potential criteria in (6), then the agent moves to it without testing other bacteria points. If the bacteria point does not meet the potential criteria then the second closest bacteria point to the target is tested. This procedure is repeated until a bacteria point meets the potential criteria in (6). When a bacteria point is selected it becomes the next point that the agent should move to. The distance between the agent and the bacteria points is constant and is determined empirically given the type of environment and the detection range of the agent's sensor.

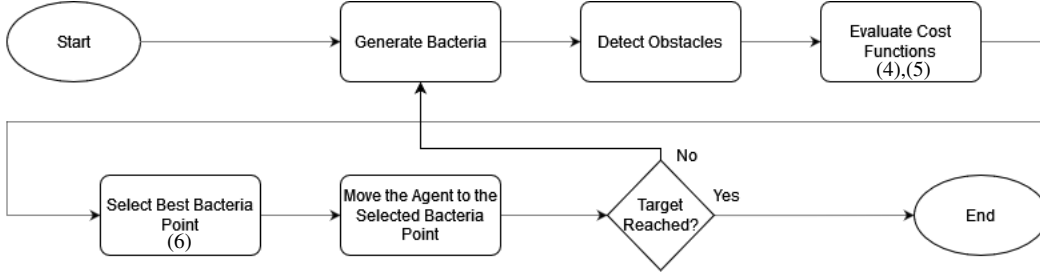


Figure 2: BAPF algorithm flow graph for agent navigation.

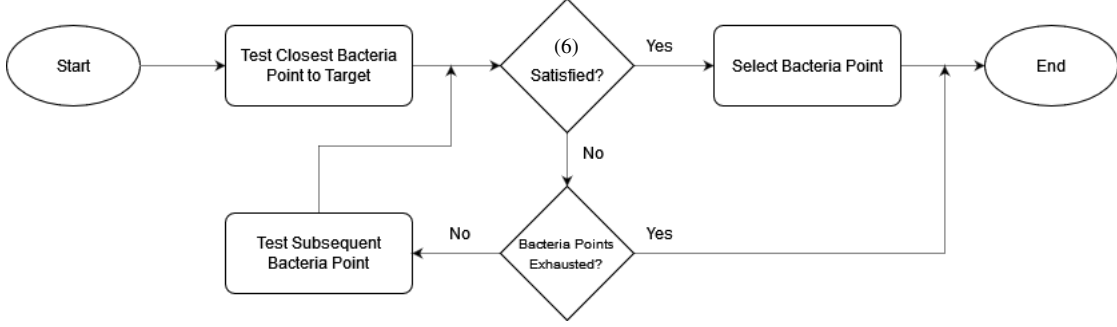


Figure 3: BAPF algorithm flow graph for best bacteria point selection.

Local Minima Trap—The major drawback of the APF methods is that they can get stuck in a local minima where the agent cannot find a solution to the problem on a certain area on the navigation region. The local minima trap is sometimes inevitable in the case of unknown environments and especially unknown cluttered environments. For the classical BAPF algorithm, the local minima trap occurs if none of the N_b bacteria points meets the criteria in (6). In this case, the agent cannot move.

To escape the local minima trap, a random walk can be employed where a bacteria point is selected randomly for the agent to move to. A strict condition for this randomly selected bacteria point is that it should not violate a minimum safety distance to a detected obstacle which will be further discussed later on. Figure 4 shows the agent escaping a local minima trap via random walk.

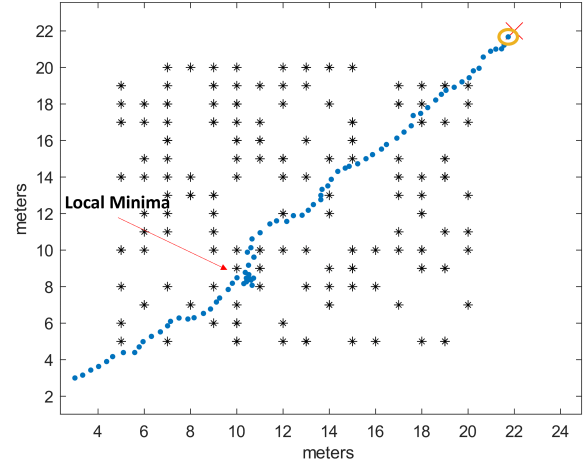


Figure 4: Local minima escape through random walk

4. IMPROVED BACTERIA APF (IBAPF) ALGORITHMS

In this section, we propose the Adaptive BAPF (A-BAPF) and the Changing Radii BAPF (CR-BAPF) algorithms to improve the performance of the classical BAPF algorithm for unknown cluttered environments.

A-BAPF Algorithm

The classical BAPF algorithm cannot achieve the best performance in unknown cluttered environments when it comes to the convergence to the target (successful navigation). Performance improvement in terms of convergence to the target can be achieved by employing our proposed A-BAPF method that is explained in this section.

The idea of A-BAPF is to adaptively choose the value of μ_o for each bacteria point by minimizing $J_k(\mathbf{r}_{b,k})$, $k = 1, 2, \dots, N_b$, in each navigation step. This can be mathemat-

ically expressed as

$$\begin{aligned} & \min_{\mu_{o,k}} J_k(\mathbf{r}_{b,k}) \\ & \text{subject to } \mu_{o,k} \in [\mu_{\min} : \mu_{\max}] \end{aligned} \quad (7)$$

where $\mu_{o,k}$, $k = 1, 2, \dots, N_b$, is the adapted parameter for the k th bacteria point. One can easily show that $J_k(\mathbf{r}_{b,k})$ in (7) is a convex function of μ_o . The solution of the minimization in (7) can be obtained by using grid search or golden-section search methods. Intuitively, when the value of μ_o approaches μ_{\max} , the repulsive potential, $J_{\text{obst}}(\mathbf{r}_{b,k})$ in (5), approaches zero and the obstacles' influence on the navigation decreases. The minimization of the potential cost function for the bacteria points can almost guarantee a solution for (6) at each navigation step and prevent the agent from ending up in a local minima. This is due to the fact that

the optimization in (7) increases the chance of that at least one bacteria point meets the condition in (6). Our proposed A-BAPF algorithm can be considered as an upper bound for the classical BAPF algorithm in terms of successful navigation performance. In the A-BAPF algorithm, the bacteria point closest to the target can be selected even if it doesn't initially meet the condition in (6). This is done by changing the value of μ_o through (7).

CR-BAPF Algorithm

While the proposed A-BAPF algorithm outperforms the classical BAPF algorithm in terms of successful navigation by avoiding the local minima trap, its computational complexity is higher compared to the classical A-BAPF because the optimization in (7) causes extra computational complexity at each navigation step. An alternative solution with lower computational complexity is the CR-BAPF algorithm.

The CR-BAPF algorithm introduces two radii around each obstacle as shown in Figure 5. For the CR-BAPF algorithm, we define the repulsive potential function from the n th detected obstacle located at $\mathbf{r}_{\text{obst}}^n = [x_{\text{obst}}^n, y_{\text{obst}}^n]^T$, $n = 1, 2, \dots, N_d$, to the agent located at $\mathbf{r} = [x, y]^T$ as

$$J_{\text{obst}}^n(\mathbf{r}) = \begin{cases} 0 & \text{if } \sqrt{\rho_{\text{obst}}^n(\mathbf{r})} > \rho_u \\ \alpha_o \exp(-\mu_o \|\mathbf{r} - \mathbf{r}_{\text{obst}}^n\|_2) & \text{if } \rho_l \leq \sqrt{\rho_{\text{obst}}^n(\mathbf{r})} \leq \rho_u \\ \infty & \text{if } \sqrt{\rho_{\text{obst}}^n(\mathbf{r})} < \rho_l \end{cases} \quad (8)$$

where $\rho_{\text{obst}}^n(\mathbf{r}) \triangleq \|\mathbf{r} - \mathbf{r}_{\text{obst}}^n\|_2^2$ is the square distance between the agent and the n th obstacle, and ρ_l and ρ_u denote the lower and upper radius, respectively. As seen in (8), if the agent's distance to the n th detected obstacle is greater than ρ_u , then the repulsive potential is zero. On the other hand, if the agent's distance to the n th obstacle is lower than ρ_l , the repulsive potential from the obstacle to the agent becomes infinity. This means that the agent does not select a bacteria point that its distance to the n th obstacle is lower than ρ_l because it does not satisfy the criteria in (6). Moreover, this also implies that the agent is not affected by obstacles that are at a greater distance than ρ_u . This way, the agent has more motion freedom in the map without risking its safety which improves the overall performance. The lower radius is meant as a safety perimeter around the obstacles to prevent collisions. The value of ρ_l is determined based on the error margin in the motion of the agent in order to prevent the agent from colliding with the obstacle. Moreover, the value of ρ_u is determined based on the estimated density of the obstacles in the navigation region. It should be mentioned that the attractive potential function to the target for the CR-BAPF is given in (1).

To further improve the performance of the proposed CR-BAPF algorithm in terms of avoiding local minima trap, we propose to employ the CR-BAPF algorithm in combination with the random walk technique. We call this new algorithm CR-BAPF*.

5. SIMULATIONS

Simulation Setup

The simulation environment is setup in MATLAB with a fixed starting position for the agent at $\mathbf{r}_s = [3, 3]^T$ and the target location at $\mathbf{r}_t = [22, 22]^T$. The location of the obstacles is considered to be a random vector $\mathbf{r}_{\text{obst}}^n = [x_{\text{obst}}^n, y_{\text{obst}}^n]^T$, $n = 1, 2, \dots, N$, uniformly distributed in a square region

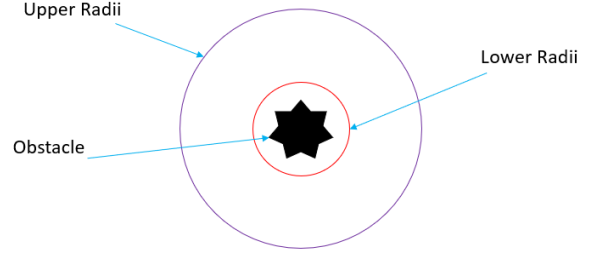


Figure 5: The upper and lower radii around a point obstacle.

Table 1: Simulation Hyperparameter Values.

Hyperparameter	Value
ρ_{rn}	8 m
α_t	10^4
μ_t	1
α_o	1
μ_o	1000
ρ_l	0.4 m
ρ_u	4.5 m

with length $L_x = 30$ m and width $L_y = 30$ m. For each Monte Carlo trial, the number of obstacles in the navigation region N is modeled by the discrete uniform random variable $N \in \mathcal{U}[20, 45]$. The considered simulation setup emulates the navigation through a set of randomly uniformly distributed obstacles such as trees or craters. The detection range is set $\rho_{rn} = 8$ m to emulate the range of an ultrasonic sensor [17], and the number of bacteria points is $N_b = 60$ to provide a rotation accuracy of 6° .

The movement step size of the agent is $\Delta r \triangleq \|\mathbf{r} - \mathbf{r}_{b,k}\|_2 = 0.4$ m, $k = 1, 2, \dots, N_b$, and the position error of the agent Δx and Δy are modeled by Gaussian distribution as $\Delta x \in 0.1\mathcal{N}(0, 1)$ and $\Delta y \in 0.1\mathcal{N}(0, 1)$. The values of the hyperparameters for $N_m = 3000$ Monte Carlo trials are given in Table 1. The upper and lower radii are considered the same for all the obstacles in the navigation region.

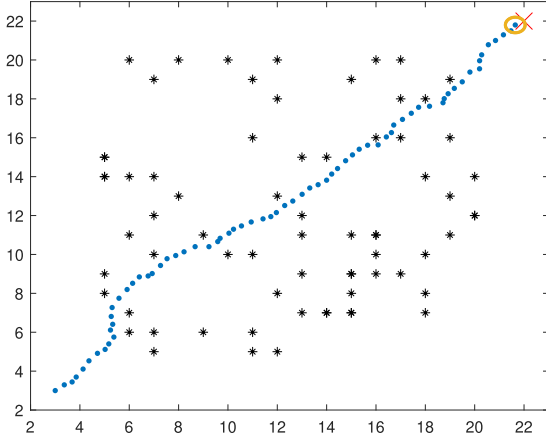
Performance Comparison Metrics

The following terms and definitions will be used in order to compare different DAA algorithms.

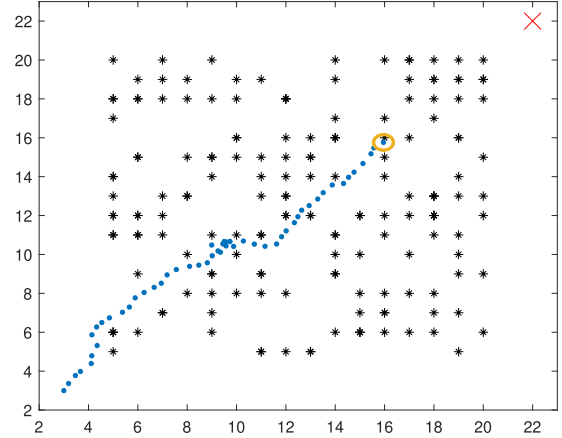
Rate of success: For N_m Monte Carlo trials, the rate of successful navigation is defined as

$$R_s \triangleq \frac{N_s}{N_m}, \quad (9)$$

where N_s denotes the number of successful navigation without getting stuck in a local minima or colliding with an obstacle.



(a) Successful navigation



(b) Unsuccessful navigation

Figure 6: Successful and unsuccessful navigation of an agent employing CR-BAPF* DAA algorithm.

Average Navigation Steps: For N_s successful navigation trials, the average navigation steps is defined as

$$\bar{M}_s = \frac{1}{N_s} \sum_{m=1}^{N_s} M_s(m), \quad (10)$$

where $M_s(m)$ is the number of navigation steps at the m th successful navigation trial.

Safety Parameter: For a successful navigation of M_s steps at locations $\mathbf{r}_1, \mathbf{r}_2, \dots, \mathbf{r}_{M_s}$ with a total of number of N unique detected obstacles during navigation, the safety parameter is the average minimum distance that the agent maintained from the detected obstacles during the navigation and is defined as

$$S \triangleq \frac{\sum_{m=1}^N \rho_{\min}(\mathbf{r}_{\text{obst}}^m)}{N}, \quad (11)$$

where $\rho_{\min}(\mathbf{r}_{\text{obst}}^m) \triangleq \min \{ \|\mathbf{r}_1 - \mathbf{r}_{\text{obst}}^m\|_2, \|\mathbf{r}_2 - \mathbf{r}_{\text{obst}}^m\|_2, \dots, \|\mathbf{r}_{M_s} - \mathbf{r}_{\text{obst}}^m\|_2 \}$ with $\mathbf{r}_{\text{obst}}^m$ is the location of the m th obstacle detected throughout the navigation.

Algorithm Complexity: The computational complexity of the DAA algorithms is evaluated in terms of average run time of the algorithm for N_m Monte Carlo trials, and it is denoted by T_a .

Simulation Results

Figure 6 shows an example of a successful navigation of the agent employing the proposed CR-BAPF* algorithm. An unsuccessful navigation where the agent gets stuck in a local minima is also shown in Figure 6. As expected, by increasing the density of the obstacles in the navigation region, the chance of successful navigation decreases.

Figure 7 illustrates the optimized value of μ_o for the selected bacteria point versus navigation step for the proposed A-BAPF algorithm. As seen, there are sharp changes in the curve because the environment the agent is moving in is a cluttered environment and thus the number of detected obstacles, the distance from the detected obstacles, and the

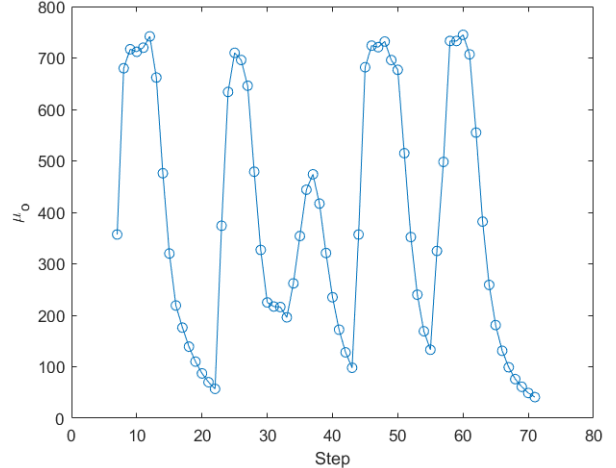


Figure 7: Optimized μ_o versus navigation step for the proposed A-BAPF algorithm.

distance from the target significantly changes during the navigation. Our simulation result show that the A-BAPF algorithm can achieve a navigation success rate of more than 95%.

Figure 8 compares the rate of success R_s versus μ_o for the proposed CR-BAPF* and the classical BAPF algorithm. As seen, the CR-BAPF* algorithm outperforms the classical BAPF algorithm for $\mu_o \in [416.67, 1000]$. The reason is that as μ_o increases, the repulsive potential from the obstacles decreases. In the BAPF algorithm, the repulsive potential depends only on the distance between the obstacle and the agent. When μ_o increases, the risk of the agent getting close to an obstacle and collision increase. However, in the CR-BAPF* algorithm there are defined perimeters around each obstacle which control the repulsive potential value and prevent the agent from getting dangerously close to an obstacle. On the other hand, for $\mu_o \in [1, 416.67]$, the repulsive potential is higher for the CR-BAPF*. This results in a higher success rate for the BAPF algorithm because it

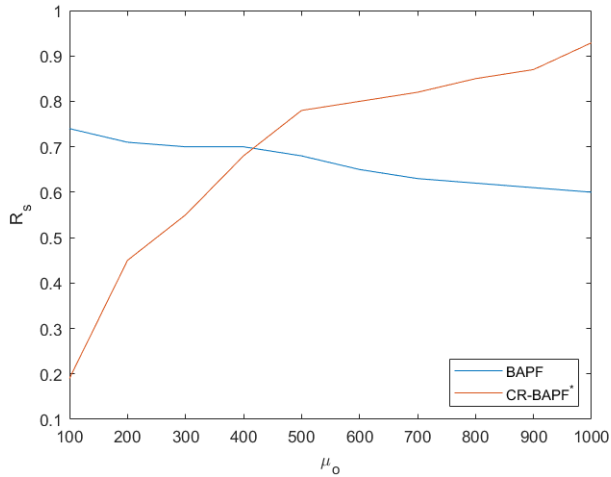


Figure 8: Rate of success R_s versus μ_o for the proposed CR-BAPF* and the classical BAPF algorithms.

Table 2: Performance Comparison

Algorithm	R_s	\bar{M}_s	S (m)	T_a (ms)
CAPF [15]	0.316	91.105	2.717	55.3
BAPF [16]	0.74	68.183	2.3763	178.3
CR-BAPF	0.827	70.77	2.358	124.2
CR-BAPF*	0.929	70.761	2.357	230.8

becomes more likely for the CR-BAPF* algorithm to reach a local minima due to the high regional repulsive potential around each obstacle.

The comparison between the CAPF, the classical BAPF, and the proposed CR-BAPF and CR-BAPF* algorithms for different performance metrics including R_s , \bar{M}_s , S , and T_a is shown in Table 2. As seen, the proposed CR-BAPF and CR-BAPF* algorithms outperform the CAPF and the classical BAPF in terms of success rate R_s . The reason is that the proposed branching repulsive potential function reduces the local minima trap and chance of collision. In terms of average navigation steps \bar{M}_s , the classical BAPF, CR-BAPF, and the CR-BAPF* algorithms exhibit similar performance and outperform the CAPF algorithm. All the four algorithms perform well when it comes to the safety criteria S because they offer $S > 2$ m on average. The CAPF algorithm has the shortest execution time, and the BAPF and CR-BAPF have longer times respectively due to the linear search performed on the bacteria points. The CR-BAPF* has the longest execution time due to the random walk implementation which imposes extra steps to get out of a local minima but yields a higher success rate. While the CAPF algorithm offers lower computational complexity compared to the classical BAPF, the CR-BAPF, and the CR-BAPF* algorithms. The latter algorithms are still considered as low complexity solutions for DAA in cluttered environments.

6. SUMMARY

We proposed the CR-BAPF DAA algorithm to solve the local minima trap problem in the classical APF algorithms. The CR-BAPF takes the advantage of a branching repulsive potential function, which results in a navigation success rate of more than 80% in highly cluttered environments. This value increases to more than 90% when the CR-BAPF algorithm is combined with the random walk technique (CR-BAPF*). Our simulation results show that the CR-BAPF algorithm offers lower navigation time compared to the CAPF similar to the classical BAPF algorithm. We established that all four algorithms maintain a good safety distance from the obstacles. Furthermore, we have shown that the execution time of all four algorithms is acceptable with the implementation of the random walk having the highest execution time in the CR-BAPF* algorithm. In addition to the CR-BAPF algorithm, we also proposed the A-BAPF algorithm that is an adaptive version of the classical BAPF algorithm and achieves the upper bound performance of the classical BAPF.

REFERENCES

- [1] Food and Agriculture Organization and the United Nations Environment Program, "The state of the world's forests 2020. forests biodiversity and people," 2020. DOI: 10.4060/ca8642en.
- [2] L. F. Oliveira, A. Moreira, and M. Silva, "Advances in forest robotics: A state-of-the-art survey," *Robotics*, vol. 10, p. 53, Mar. 2021. DOI: 10.3390/robotics10020053.
- [3] A. Mustain. (Jun. 2011). "Mysteries of the oceans remain vast and deep," [Online]. Available: <https://www.livescience.com/14493-ocean-exploration-deep-sea-diving.html>.
- [4] J. N. Yasin, S. A. S. Mohamed, M.-H. Haghbayan, J. Heikkonen, H. Tenhunen, and J. Plosila, "Unmanned aerial vehicles (uavs): Collision avoidance systems and approaches," *IEEE Access*, vol. 8, 2020, pp. 105 139–105 155, Jun. 2020. DOI: 10.1109/ACCESS.2020.3000064.
- [5] N. Gageik, P. Benz, and S. Montenegro, "Obstacle detection and collision avoidance for a uav with complementary low-cost sensors," *IEEE Access*, vol. 3, pp. 599–609, 2015.
- [6] J. Seo, Y. Kim, S. Kim, and A. Tsourdos, "Collision avoidance strategies for unmanned aerial vehicles in formation flight," *IEEE Transactions on Aerospace and Electronic Systems*, vol. 53, no. 6, pp. 2718–2734, 2017. DOI: 10.1109/TAES.2017.2714898.
- [7] M. Wang, H. Voos, and D. Su, "Robust online obstacle detection and tracking for collision-free navigation of multirotor uavs in complex environments," *Proc. 15th Int. Conf. Control, Automat., Robot. Vis. (ICARCV)*, pp. 1228–1234, Nov. 2018.
- [8] D. Bareiss and J. van den Berg, "Reciprocal collision avoidance for robots with linear dynamics using lqr-obstacles," in *2013 IEEE International Conference on Robotics and Automation*, 2013, pp. 3847–3853. DOI: 10.1109/ICRA.2013.6631118.
- [9] S. Hrabar, "Reactive obstacle avoidance for rotorcraft uavs," in *2011 IEEE/RSJ International Conference on Intelligent Robots and Systems*, 2011, pp. 4967–4974. DOI: 10.1109/IROS.2011.6094629.
- [10] P. Conroy, D. Bareiss, M. Beall, and J. Berg, "3-d reciprocal collision avoidance on physical quadrotor

helicopters with on-board sensing for relative positioning,” Nov. 2014.

- [11] S. Roelofsen, D. Gillet, and A. Martinoli, “Reciprocal collision avoidance for quadrotors using on-board visual detection,” in *2015 IEEE/RSJ International Conference on Intelligent Robots and Systems (IROS)*, 2015, pp. 4810–4817. DOI: 10.1109/IROS.2015.7354053.
- [12] J. Sun, J. Tang, and S. Lao, “Collision avoidance for cooperative uavs with optimized artificial potential field algorithm,” *IEEE Access*, vol. 5, pp. 18 382–18 390, 2017. DOI: 10.1109/ACCESS.2017.2746752.
- [13] C. Randell, C. Djiallis, and H. Muller, “Personal position measurement using dead reckoning,” Nov. 2005, pp. 166–173, ISBN: 0-7695-2034-0. DOI: 10.1109/ISWC.2003.1241408.
- [14] O. Khatib, “Real-time obstacle avoidance for manipulators and mobile robots,” *Int. Conf. Robot. Automat.*, vol. 2, pp. 500–505, Mar. 1985.
- [15] J. C. Mohanta, D. R. Parhi, S. K. Patel, and S. K. Pradhan, “Real-time motion planning of multiple mobile robots using artificial potential field method,” *Journal of Advance Computational Research*, vol. 01, Jan. 2016.
- [16] Y. Ahmad. (May 2020). “Matlab implementation of artificial potential field,” [Online]. Available: <https://github.com/Yaaximus/artificial-potential-field-matlab>.
- [17] B. Roderick. (Mar. 2020). “Understanding how ultrasonic sensors work,” [Online]. Available: <https://www.maxbotix.com/articles/how-ultrasonic-sensors-work.htm>.